

1 **SECOND ORDER FINITE VOLUME IMEX NUMERICAL METHODS**
2 **FOR OPTION PRICING***

3 J.G. LÓPEZ-SALAS ^{*†}, M. SUREZ-TABOADA [†], M.J. CASTRO[‡], A.M.
4 FERREIRO-FERREIRO [†], AND J.A. GARCÍA-RODRÍGUEZ [†]

5 **Abstract.** This article deals with the development of second order finite volume numeri-
6 cal schemes for solving option pricing problems, modelled by low dimensional advection-diffusion-
7 reaction scalar partial differential equations. These equations will be discretized using second order
8 finite volume Implicit-Explicit (IMEX) Runge-Kutta schemes. The developed methods will be able
9 to overcome the time step restriction due to the strict stability condition of parabolic problems with
10 diffusion terms. Besides, the schemes will offer high-accurate and non oscillatory approximations of
11 option prices and their Greeks.

12 **Key words.** Option pricing, finite volume method, advection-diffusion, IMEX Runge-Kutta.

13 **1. Introduction.** Mathematical models for option pricing play a key role in the
14 financial industry. An option is a contract that gives the right to buy or sell some
15 underlying asset at a future date, for an agreed price. The price of the underlying
16 asset is modelled via stochastic processes. These processes are described by stochastic
17 differential equations (SDEs) or systems of SDEs. The value of an option at expiration
18 is given by its payoff function. The expected present value of this payoff function is
19 the option price before its maturity.

20 Monte Carlo simulation is the straightforward choice for computing numerically
21 the expectation defining the option price. This numerical method has many advan-
22 tages. The fact that its order of convergence is independent of the dimension of the
23 problem represents its major strength. Besides, the method allows to easily price
24 options with sophisticated payoffs and complex models for the underlyings. Nev-
25 ertheless, Monte Carlo simulation has also several drawbacks. Firstly, its order of
26 convergence is $O(\frac{1}{\sqrt{S}})$, being S the number of Monte Carlo simulations. Thus, the
27 method is very slow, since a large number of simulations are needed to get an accurate
28 price. Secondly, the explicit evaluation of the expectation is very difficult for options
29 with early-exercise features (American-style options). Besides, the computation of
30 derivatives of option prices, the so-called Greeks, presents theoretical and practical
31 challenges to Monte Carlo simulation. Finally, pricing barrier options by means of
32 Monte Carlo simulation requires the use of the complex Brownian bridge techniques.

33 Feynman-Kac formula establishes a connection between SDEs and partial differ-
34 ential equations (PDEs). Therefore, the option price given by the expected present
35 value of its payoff can be computed by solving PDEs with classical numerical meth-

*Submitted to the editors December 5, 2021.

Funding: The third author research has been partially supported by the Spanish Govern-
ment and FEDER through the coordinated Research project RTI2018-096064-B-C1, the Junta de
Andalucía research project P18-RT-3163, the Junta de Andalucía-FEDER-University of Málaga re-
search project UMA18-FEDERJA-16 and the University of Málaga. The other authors research
has been partially supported by the Spanish MINECO under research project number PDI2019-
108584RB-I00. As members of CITIC, they also acknowledge the grant ED431G 2019/01, funded by
Consellería de Educación, Universidade e Formación Profesional of Xunta de Galicia and FEDER.

[†]Department of Mathematics and CITIC, University of A Coruña, Faculty of Informatics,
Campus Elviña s/n, A Coruña, 15071, Galicia, Spain (jose.lsalas@udc.es, maria.suarez3@udc.es,
ana.ferreiro@udc.es, jagrodriguez@udc.es).

[‡]Department of Análisis Matemático, Facultad de Ciencias, University of Málaga, Campus de
Teatinos s/n, Málaga, 29080, Andaluca, Spain (mjcastro@uma.es).

36 ods like finite differences, finite elements or finite volumes. Although these methods
 37 suffer the curse of dimensionality, they offer several advantages: solvers with high-
 38 order of convergence can be developed, the computation of the Greeks is straight-
 39 forward, American options can be easily priced and exotic derivatives like barrier
 40 options fit very naturally in the PDE context, where only boundary conditions need
 41 to be changed. In this article we will develop deterministic numerical methods for
 42 solving Black-Scholes PDEs in low dimension. These are advection-diffusion-reaction
 43 scalar PDEs, with the following general expression in dimension one

$$44 \quad (1.1) \quad \frac{\partial u}{\partial t} + a(x, t) \frac{\partial u}{\partial x} + b(x, t) \frac{\partial^2 u}{\partial x^2} + c(x, t)u = 0.$$

45 The discretization of these kind of financial PDEs with finite difference and finite ele-
 46 ment methods is discussed in [9, 29, 1, 22]. The combination of finite differences with
 47 Exponentially Fitted techniques is explained in [10]. Besides, Alternate Directions
 48 (ADI) with finite differences is illustrated in [12].

49 However, the development of finite difference and finite element numerical meth-
 50 ods for PDEs arising in mathematical finance presents several well known difficulties.
 51 First, and most important, these numerical methods usually show instabilities when
 52 the advection term becomes larger and/or the diffusion operator is degenerated. Up-
 53 winding techniques are needed to overcome this issue. Secondly, the development of
 54 high order pricers is challenging, because second order (or higher) convergence is lost
 55 when the initial condition is not regular: this is precisely the usual situation in option
 56 pricing, as the initial condition is given by a payoff function that is usually singu-
 57 lar. Finally, another difficulty, derived from the previous ones, is achieving accurate
 58 and non oscillatory approximations of the Greeks. The derivatives of the solution
 59 are usually computed by means of finite difference formulas, which are very sensitive
 60 to small errors in the approximation of the prices. The higher the derivatives the
 61 more difficult is obtaining approximations without oscillations. This question is of
 62 paramount importance, since the Greeks are vital for trading purposes. Developing
 63 very accurate and high order schemes is a key step towards attaining non-fluctuating
 64 approximations of the Greeks.

65 In order to avoid the problems originated by non-smooth payoffs, smoothing tech-
 66 niques working on irregular initial data were proposed in the literature, see [28]. One
 67 remarkable smoothing technique is the so-called Rannacher's method, see [18]. It is
 68 well known that the second order Crank-Nicolson time marching scheme loses order
 69 when initial conditions are non-smooth, or the initial and boundary conditions are
 70 discontinuous, which is the situation with barrier options. Rannacher proposed a
 71 way to suppress wrongful initial oscillations, by preceding Crank-Nicolson with a few
 72 implicit steps.

73 Additionally, several numerical strategies were presented in the literature in order
 74 to overcome the problems emerging in convection dominated scenarios. One approach
 75 is the method of characteristics. In [8], Forsyth et al. solve option pricing problems
 76 with finite differences combined with the semi-Lagrangian characteristics method. In
 77 the finite element setup, semi-Lagrangian characteristics was applied in [2] for pricing
 78 Asian options. In [7] the authors present a semi-Lagrangian finite difference method
 79 for pricing business companies. The main disadvantages of semi-Lagrangian meth-
 80 ods in option pricing is the difficulty to build high order numerical schemes. In fact,
 81 these numerical methods do not achieve second order convergence due to the non-
 82 smoothness of either the payoff or the boundary conditions. On top of that, the
 83 computational cost of characteristic method is high due to the demanding compu-

84 sory search at the foot of the characteristic and the required interpolation. Another
85 approach for a better treatment of the advection terms is the use of finite volume
86 methods. The first work applying finite volume methods in option pricing problems
87 was [32]. Later, in [23] conservative explicit finite volume methods were proposed for
88 convection dominated pricing problems. More precisely, the authors propose to use
89 the extension of the central schemes presented by Nessyahu-Tadmor in [20] to the
90 advection-diffusion problem developed in [15]. Recently, in [4], the authors propose a
91 second order improvement to [23] with appropriate time methods and slope limiters.
92 In [3] the authors apply the explicit third order Kurganov-Levy scheme presented
93 in [14] along with the CWENO reconstructions presented in [17]. In all these arti-
94 cles, it is shown that explicit finite volume schemes do not suffer loss in the order of
95 convergence. Besides, they are able to obtain approximations of the Greeks without
96 oscillations. Nevertheless, these works present numerical schemes explicit in time.
97 Explicit time integrators introduce a severe restriction in the time step, imposed by
98 the Von Neuman stability condition related to the diffusion terms. As a consequence,
99 these schemes have a huge computational cost and are not able in practice to work
100 with refined meshes in space, specially in problems with spatial dimension greater
101 than one.

102 In this work we develop finite volume numerical solvers for option pricing problems
103 in low dimension. The proposed schemes address the mentioned problems of finite
104 difference and finite element methods, while at the same time retain a large time step
105 in the time discretization. More precisely, we present a general technique, following
106 [21, 6], for building second-order Implicit-Explicit (IMEX) Runge-Kutta finite volume
107 solvers for option pricing. This numerical scheme allows to use different numerical
108 flux functions and opens the door to the consideration of high order reconstructions
109 in mathematical finance. The proposed method is able to overcome the severe time
110 step restriction thanks to the implicit treatment of the diffusive part, while retaining
111 at the same time the benefits of treating the advective term by means of a explicit
112 finite volume scheme. In this way the stability condition of the IMEX scheme allows
113 to use the same time step of the advective part, which is far larger than the diffusive
114 time step. Moreover, finite volume schemes allow to address the lost of order of
115 convergence when initial data is non-smooth, since they handle the integral version
116 of the equations, working with the averaged solutions in each cell. Consequently, true
117 second order schemes are proposed for option pricing problems, that also allow to
118 recover accurate and non oscillatory approximations of the Greeks.

119 The organization of this paper is as follows. In the Section 2 we review Black-
120 Scholes PDEs and vanilla, butterfly, barrier and Asian options. In Section 3 we
121 describe the proposed finite volume IMEX Runge-Kutta numerical scheme. In Sec-
122 tion 4, we present the numerical experiments that we have carried out. We validate
123 the numerical scheme by pricing options with known analytical solution. More pre-
124 cisely, Section 4.1 is devoted to price vanilla, butterfly and barrier options under the
125 classical Black-Scholes model. All these options are priced by means of solving the
126 one dimensional Black-Scholes PDE with different terminal conditions. In Section 4.2
127 a two dimensional problem is considered: Asian options are valued by solving a two
128 dimensional Black-Scholes PDE without crossed derivatives. Asian PDEs are solved
129 by extending the one dimensional numerical schemes using the method of lines.

130 **2. Option pricing PDE models.** A financial derivative is a contract whose
131 value depends on the evolution of the price of one or more assets, called underlying
132 assets. An option is a kind of derivative consisting of a contract between two parties

133 about trading a risky asset at a certain future time, or within a specified period of
 134 time, given by the exercise date or maturity (T). One party is the seller of the option,
 135 who fixes the terms of the contract, and gives to the option's holder the right (and
 136 not the obligation) to buy (call option) or sell (put option) a particular asset at a
 137 fixed price. This price is agreed on beforehand, and it is known as exercise price or
 138 strike (K).

139 Options are mainly characterized by the payoff function and the kind of allowed
 140 exercise. Call and put options, also called vanilla options, are the simplest ones. On
 141 the other hand, the so-called exotic options, have very complicated structures. An
 142 option is called path-dependent when its payoff depends explicitly on the values of
 143 the underlying asset at multiple dates before expiration. Examples of path dependent
 144 options are the barrier and Asian options. An option is called European if exercise is
 145 only permitted at maturity, and is called American if it can be exercised at any time
 146 before expiry.

147 Determining the fair price of the option, the so-called premium, at the time of
 148 the contract signature is an important financial problem. This is the subject of the
 149 present work. More precisely, we will focus on pricing several European-style options:
 150 vanilla options and exotic options (barrier and Asian options). For the dynamics of the
 151 underlying asset we will consider the Black-Scholes model, which is briefly introduced
 152 below.

153 **2.1. Black-Scholes model.** Let us now consider the Black-Scholes option pricing
 154 model presented in the articles by Merton [19] and Black and Scholes [5]. The
 155 model describes the evolution of the risky asset through the following SDE

$$156 \quad (2.1) \quad \frac{ds_t}{s_t} = (r - q)dt + \sigma dW_t,$$

157 with W_t a standard Brownian motion. The parameter $r \in \mathbb{R}$ is the risk free constant
 158 interest rate and $q \in \mathbb{R}$ is the continuous dividend yield. This SDE implicitly describes
 159 the risk-neutral dynamics of the underlying asset price, since the coefficient on dt in
 160 (2.1), the so-called mean rate of return, is considered as $r - q$. The parameter $\sigma \in \mathbb{R}^+$
 161 is the volatility of the stock price, which is again considered as constant. BlackScholes
 162 model is based on several assumptions, like for example the fact that the volatility of
 163 the underlying asset is a deterministic constant (see [29] for details on all assumptions).
 164 Although nowadays all of these assumptions about the market can be shown wrong
 165 up to a certain extent, the Black-Scholes model is still very important in theory and
 166 practice, and it has a huge impact on financial markets.

The SDE (2.1) has analytical solution which can be expressed as

$$s_T = s_0 \exp \left(\left(r - q - \frac{1}{2} \sigma^2 \right) T + \sigma W_T \right),$$

167 where s_0 is the known current price of the underlying asset, and W_T is a random
 168 variable normally distributed with mean 0 and variance T . Therefore, the asset price
 169 has a lognormal distribution. For some payoffs, like those of vanilla options, the
 170 expected present value of the payoff of the option, which is an integral with respect to
 171 the lognormal density of s_T , can be analytically computed, giving rise to the celebrated
 172 Black-Scholes formulas for the prices of call and put options.

173 The price u of any option on the underlying s is fully determined at every instant
 174 t by the asset value s_t . Hence, the value of the option is a function $u(s, t)$. Applying
 175 It's lemma (see [27], for example), one can derive the SDE for u . In order to comply

176 with the no-arbitrage conditions, the process du has to be martingale. Therefore,
 177 the drift term of the SDE for u must be zero, which implies the well-known linear
 178 parabolic backward in time Black-Scholes PDE

$$179 \quad (2.2) \quad \frac{\partial u}{\partial t} + \frac{1}{2}\sigma^2 s^2 \frac{\partial^2 u}{\partial s^2} + (r - q)s \frac{\partial u}{\partial s} - ru = 0, \quad (s, t) \in [0, \infty) \times [0, T].$$

180 Hereafter, in this work we will work forward in time by making the change of variable
 181 $\tau = T - t$ in (2.2). By abuse of notation this forward time τ is again written as t , so
 182 that forward in time Black-Scholes PDE is

$$183 \quad (2.3) \quad \frac{\partial u}{\partial t} - \frac{1}{2}\sigma^2 s^2 \frac{\partial^2 u}{\partial s^2} - (r - q)s \frac{\partial u}{\partial s} + ru = 0, \quad (s, t) \in [0, \infty) \times [0, T].$$

184 PDE (2.3) must be completed with initial and boundary conditions. The initial con-
 185 dition $u(s, 0)$ depends on the payoff of the option and the boundary conditions should
 186 be carefully determined taking into account financial aspects as well as mathematical
 187 questions. Throughout the next subsections several types of options will be described,
 188 together with their corresponding initial and boundary conditions.

189 **2.1.1. Vanilla options.** A European call option is the right to buy a risky asset
 190 at a fixed strike price K only at the future time T (measured in years). The call option
 191 holder would exercise the option at expiry if the asset price is above the strike K and
 192 not if it is below. Therefore, the payoff of a call option is $s_T - K$ if $s_T > K$ and 0
 193 otherwise. Thus, the payoff of a European call option is $\max(s_T - K, 0)$. Conversely,
 194 a put option gives the right to sell. At expiry the option is worth $\max(K - s_T, 0)$.
 195 Therefore, the initial condition of (2.3) is $u(s, 0) = \max(s - K, 0)$ for call options and
 196 $u(s, 0) = \max(K - s, 0)$ for put options.

In order to solve numerically the Black-Scholes PDE we need to truncate the
 spatial domain. Therefore u will be computed for $s \in (0, \bar{s})$, with \bar{s} large enough.
 Besides, boundary conditions have to be imposed at the boundaries. For call options
 the following Dirichlet boundary conditions can be used

$$u(0, t) = 0, \quad u(\bar{s}, t) = \bar{s}e^{-qt} - Ke^{-rt},$$

while for put options

$$u(0, t) = Ke^{-rt} - \bar{s}e^{-qt}, \quad u(\bar{s}, t) = 0.$$

197 The analytical solutions for European call and put options are given by (see
 198 [5, 19])

$$199 \quad (2.4) \quad C(s, K, t) = se^{-qt}N(d_1(s, K)) - Ke^{-rt}N(d_2(s, K)),$$

$$200 \quad (2.5) \quad P(s, K, t) = Ke^{-rt}N(-d_2(s, K)) - se^{-qt}N(-d_1(s, K)),$$

201 where N is the cumulative distribution function of the standard normal distribution,
 202 and d_1, d_2 are defined as

$$203 \quad (2.6) \quad d_1(s, K) = \frac{1}{\sigma\sqrt{t}} \left[\ln\left(\frac{s}{K}\right) + \nu t \right], \quad \nu = r - q + \frac{\sigma^2}{2},$$

$$204 \quad (2.7) \quad d_2(s, K) = d_1(s, K) - \sigma\sqrt{t}.$$

206 The delta of an option is the sensitivity of the option to a change in the underlying
 207 asset, $\Delta = \frac{\partial u}{\partial s}$. The gamma of an option, Γ , is the sensitivity of the delta to the

208 underlying, $\Gamma = \frac{\partial^2 u}{\partial s^2}$. For call and put options under the Black-Scholes model, Greeks
209 are known in closed form

$$210 \quad (2.8) \quad \Delta_C(s, K, t) = e^{-qt} N(d_1(s, K)), \quad \Gamma_C(s, K, t) = \frac{e^{-qt} n(d_1(s, K))}{s\sigma\sqrt{t}},$$

$$211 \quad (2.9) \quad \Delta_P(s, K, t) = -e^{-qt} N(-d_1(s, K)), \quad \Gamma_P(s, K, t) = \Gamma_C(s, K, t),$$

213 where $n(x) = \frac{e^{-x^2/2}}{\sqrt{2\pi}}$ is the probability density function of the standard normal
214 distribution.

2.1.2. Butterfly spread. A butterfly spread is a financial product which involves buying two calls with strike prices K_1 and K_3 and selling two calls with strike price $K_2 = \frac{1}{2}(K_1 + K_3)$, where $K_1 < K_2 < K_3$. In this case, Black-Scholes PDE (2.3) is completed with the initial condition

$$u(s, 0) = \max(s - K_1, 0) + \max(s - K_3, 0) - 2 \max\left(s - \frac{1}{2}(K_1 + K_3), 0\right),$$

215 and with homogeneous Dirichlet boundary conditions $u(0, t) = u(\bar{s}, t) = 0$.

The price of the butterfly spread is also known analytically and is given by

$$u(s, t) = C(s, K_1, t) + C(s, K_3, t) - 2C(s, K_2, t),$$

216 where C is the price of the call option given in (2.4). Thus, the Greeks of the but-
217 tterfly spread can be computed in closed form as a linear combination of the Greeks
218 associated to the call options involved in the financial product.

219 **2.1.3. Barrier options.** Barrier options are exotic path-dependent options.
220 One example of barrier options is the down-and-out call option. This derivative pays
221 $\max(s - K, 0)$ at expiry, unless at any previous time the underlying asset touched
222 or crossed a prespecified level B , called the barrier. In that situation the option be-
223 comes worthless. There are also *in* options which only pays off if the asset reached or
224 crossed the barrier, otherwise they expire worthless. These barrier options are called
225 continuously monitored barrier options.

A down-and-out call option under Black-Scholes model can be priced solving PDE (2.3) with initial condition

$$u(s, 0) = \begin{cases} \max(s - K, 0) & \text{for } s > B, \\ 0 & \text{for } s \leq B, \end{cases}$$

226 in the localized domain $(s, t) \in [B, \bar{s}] \times (0, T]$ with the boundary conditions $u(B, t) = 0$
227 and $u(\bar{s}, t) = se^{-qt} - Ke^{-rt}$ for $t \in (0, T]$. Due to the sharp discontinuity arising at
228 the barrier this option is mathematically interesting in the PDE world. We will price
229 this product with our proposed finite volume IMEX Runge-Kutta schemes.

230 Standard European continuously monitored barrier options can be priced in closed
231 form. Their Greeks can be also computed analytically. In [19], Merton provides for
232 first time such formulas. See also [25, 24, 30, 26]. Hereafter we are going to detail
233 these formulas for down-and-in call options. Formulas for down-and-out call options
234 can be inferred using that a portfolio consisting of an in option and its corresponding
235 out option has the same price and Greeks of the corresponding vanilla option, i.e
236 $C(s, K, t) = C_{DO}(s, K, t) + C_{DI}(s, K, t)$. All these formulas are needed in order to

237 measure the accuracy and the order of convergence of the proposed numerical schemes.
 238 Greek formulas are carefully detailed below since we were not able to find them in
 239 the literature.

240 Let $\bar{K} = \max(B, K)$ and let $\lambda = \frac{2}{\sigma^2}(r - q - \frac{\sigma^2}{2})$. The price of the down-and-in
 241 call option is given by:

$$242 \quad C_{DI}(s, K, t) = \left(\frac{B}{s}\right)^\lambda \left[C\left(\frac{B^2}{s}, \bar{K}, t\right) + (\bar{K} - K)N\left(d_1\left(\frac{B^2}{s}, \bar{K}\right)\right) \right]$$

$$243 \quad (2.10) \quad + \left[P(s, K, t) - P(s, B, t) + \frac{(B - K)e^{-rt}}{\sigma s \sqrt{t}} N[-d_1(s, B)] \right] \mathbb{1}_{B > K}.$$

244 Hereafter we compute the delta and the gamma Greeks for the down-and-in call
 245 option. In the following expressions, for sake of brevity, in the formulas of the prices
 246 and deltas of vanilla call and put options, the time t dependency is omitted. The
 247 delta of the down-and-in call option can be computed by deriving (2.10) with respect
 248 to s , and is given by

$$249 \quad (2.11) \quad \Delta_{DI} = \frac{\Upsilon B^\lambda}{s^{\lambda+1}} + \left(\Delta_P(s, K) - \Delta_P(s, B) - \frac{(B - K)e^{-rt}}{\sigma s \sqrt{t}} n[-d_1(s, B)] \right) \mathbb{1}_{B > K},$$

250 where

$$251 \quad \Upsilon = -\lambda C\left[\frac{B^2}{s}, \bar{K}\right] - \frac{B^2}{s} \Delta_C\left[\frac{B^2}{s}, \bar{K}\right]$$

$$252 \quad - (\bar{K} - K)e^{-rt} \left\{ \lambda N\left[d_1\left(\frac{B^2}{s}, \bar{K}\right)\right] + \frac{1}{\sigma \sqrt{t}} n\left[d_1\left(\frac{B^2}{s}, \bar{K}\right)\right] \right\}.$$

253 Again, differentiating in (2.11) with respect to s , the gamma of the down-and-in
 254 call option is given by

$$255 \quad \Gamma_{DI} = -\frac{\Upsilon B^\lambda (\lambda + 1)}{s^{\lambda+2}} + \frac{\Psi B^\lambda}{s^{\lambda+1}} +$$

$$256 \quad (2.12) \quad \left[\Gamma_P(s, K) - \Gamma_P(s, B) + \frac{(B - K)e^{-rt}}{\sigma s^2 \sqrt{t}} \left(n[-d_1(s, B)] + \frac{1}{\sigma \sqrt{t}} n'[-d_1(s, B)] \right) \right] \mathbb{1}_{B > K},$$

258 where

$$259 \quad \Psi = \frac{B^2}{s^2} \left((\lambda + 1) \Delta_C\left[\frac{B^2}{s}, \bar{K}\right] + \frac{B^2}{s} \Gamma_C\left[\frac{B^2}{s}, \bar{K}\right] \right)$$

$$260 \quad + \frac{(\bar{K} - K)e^{-rt}}{\sigma s \sqrt{t}} \left(\lambda n\left[d_1\left(\frac{B^2}{s}, \bar{K}\right)\right] + \frac{1}{\sigma \sqrt{t}} n'\left[d_1\left(\frac{B^2}{s}, \bar{K}\right)\right] \right).$$

261 Finally, note that the delta and the gamma of the down-and-out call option can
 262 be obtained as $\Delta_{DO} = \Delta_C - \Delta_{DI}$ and $\Gamma_{DO} = \Gamma_C - \Gamma_{DI}$.

263 **2.1.4. Asian options.** Asian options are path dependent options whose payoff
 264 depends on the price s_T of the risky asset and also on the arithmetic average price
 265 a_T of the price s_t defined by $a_t = \frac{1}{t} \int_0^t s_\tau d\tau$. Different types of Asian options are
 266 traded in financial markets. Floating strike call options have the payoff function
 267 $\max(s_T - a_T, 0)$, while fixed strike call options consider the payoff $\max(a_T - K, 0)$,
 268 being K the strike price. American-style Asian options are also negotiated.

269 Let us denote by $u(s, a, t)$ the price of an Asian option. Under the standard
 270 Black-Scholes model for the risky asset, one can check that the price of an Asian
 271 option with payoff function $u_0(s, a)$ is the solution of the following forward in time
 272 two dimensional PDE (see [31])

$$273 \quad (2.13) \quad \frac{\partial u}{\partial t} - \frac{1}{2}\sigma^2 s^2 \frac{\partial^2 u}{\partial s^2} - rs \frac{\partial u}{\partial s} - \frac{1}{T-t}(s-a) \frac{\partial u}{\partial a} + ru = 0, \quad u(s, a, 0) = u_0(s, a).$$

274 As an example, $u_0(s, a) = \max(a - K, 0)$ is the initial condition for an European fixed
 275 strike call option.

276 For European or American floating strike options, in [13] Ingersoll reduced PDE
 277 (2.13) to a one-dimensional PDE under a suitable change of variable. For European
 278 Asian options, both fixed and floating strike, in [16], Rogers and Shi showed that
 279 the value of the Asian option is governed by an alternative one dimensional PDE.
 280 Nevertheless, in order to value American-style fixed strike options, one can not use
 281 one dimensional models, and has to solve the two dimensional PDE (2.13). For this
 282 reason, in this work we restrict ourselves to the general two dimensional framework
 283 (2.13). Analytical solutions are not known, except for the case of fixed strike options
 284 with $K = 0$.

285 PDE (2.13) has no diffusion in the a variable, thus this equation is difficult to solve
 286 numerically. In fact, the convective term in the a direction increases as t approaches
 287 T . At $t = T$, PDE (2.13) has a singularity because of the $\frac{1}{T-t}(s-a) \frac{\partial u}{\partial a}$ term. For
 288 fixed strike options, the singularity can be avoided considering $s = a$ at $t = T$. Under
 289 this assumption, (2.13) reduces to Black-Scholes equation (2.3) at $t = T$.

290 In the Section 4 of the numerical experiments we will price a European-style
 291 Asian fixed strike call option. PDE (2.13) will be solved in the localized domain
 292 $(s, a, t) \in (0, \bar{s}) \times (0, \bar{a}) \times (0, T]$ (usually $\bar{s} = \bar{a}$) with the following boundary condition
 293 $\frac{\partial^2 u}{\partial s^2}(\bar{s}, a, t) = 0$. The other portions of the boundary do not require the prescription
 294 of boundary conditions. Since the convective term in the a direction depends on
 295 time, once the problem is discretized, the matrices of the resulting systems have to
 296 be computed and inverted at each time step.

297 **3. Numerical methods. Finite volume IMEX Runge-Kutta.** In this sec-
 298 tion we present a second order finite volume semi-implicit numerical scheme for solving
 299 (2.3). First, the equation (2.3) must be written in conservative form:

$$300 \quad (3.1) \quad \frac{\partial u}{\partial t} + \frac{\partial}{\partial s} f(u) = \frac{\partial}{\partial s} g(u_s) + h(u).$$

301 The numerical solution of equation (3.1) using a explicit finite volume scheme may
 302 have a huge computational cost because of the tiny time steps induced by the diffusive
 303 terms. To avoid this difficulty we consider IMEX Runge-Kutta methods (see [21]).
 304 These methods play a major rule in the treatment of differential systems governed by
 305 stiff and non stiff terms.

306 The procedure for obtaining the numerical scheme can be summarized as follows.
 307 First, we perform a spatial finite volume semi-discretization of (3.1), explicit in con-
 308 vection and reaction, and implicit in the diffusive part. As a result we obtain a stiff
 309 time ODE system, that we discretize using IMEX Runge-Kutta methods. In what
 310 follows we succinctly describe the space and time discretizations.

311 **3.1. Spatial semi-discretization. Finite volume method.** The spatial semi-
 312 discretization of the advective and source terms is performed by means of a explicit

313 finite volume scheme. First, a finite volume mesh is built. The spatial domain is split
 314 into cells (finite volumes) $\{I_i\}$, with $I_i = [s_{i-1/2}, s_{i+1/2}]$, $i = \dots, -1, 0, 1, \dots$, being
 315 s_i the center of the cell I_i . Let $|I_i|$ be the size of cell I_i . The basic unknowns of our
 316 problem are the averages of the solution $u(s, t)$ in the cells $\{I_i\}$, $\bar{u}_i = \frac{1}{|I_i|} \int_{I_i} u ds$. In-
 317 tegrating equation (3.1) in space on I_i and dividing by $|I_i|$ we obtain the semi-discrete
 318 equation

$$319 \quad (3.2) \quad \frac{d\bar{u}_i}{dt} = - \frac{1}{|I_i|} [f(u(s_{i+1/2}, t)) - f(u(s_{i-1/2}, t))]$$

$$320 \quad (3.3) \quad + \frac{1}{|I_i|} [g(u_s(s_{i+1/2}, t)) - g(u_s(s_{i-1/2}, t))]$$

$$321 \quad (3.4) \quad + \frac{1}{|I_i|} \int_{I_i} h(u) ds.$$

323 Then, the right hand side of this expression (3.2)-(3.4) is approximated with a function
 324 of the cell averages $\{\bar{u}_i(t)\}_i$.

The convective terms in (3.2) can be approximated by solving the Riemann prob-
 lems at the edge of the cells using a suitable numerical flux function \mathcal{F} consistent with
 the analytical flux f , i.e.

$$f(u(s_{i\pm 1/2}, t)) \approx \mathcal{F}(u_{i\pm 1/2}^-, u_{i\pm 1/2}^+).$$

325 Thus one obtains

$$326 \quad f(u(s_{i+1/2}, t)) - f(u(s_{i-1/2}, t)) \approx \mathcal{F}(u_{i+1/2}^-, u_{i+1/2}^+) - \mathcal{F}(u_{i-1/2}^-, u_{i-1/2}^+).$$

The quantities $u_{i\pm 1/2}^\pm$ are computed as

$$u_{i\pm 1/2}^\pm = \lim_{s \rightarrow s_{i\pm 1/2}^\pm} \mathcal{R}(s),$$

where \mathcal{R} is a reconstruction of the unknown function $u(s, t)$. More precisely, \mathcal{R} is
 given by a piecewise polynomial starting from cell averages $\{\bar{u}_i(t)\}$,

$$\mathcal{R}(s) = \sum_i P_i(s) \mathbf{1}_{s \in I_i},$$

328 where P_i is a polynomial satisfying some accuracy and non oscillatory property, and
 329 $\mathbf{1}_{s \in I_i}$ is the indicator function of cell I_i . For second order schemes, the reconstruction
 330 have to be at least piecewise linear.

In this work for the numerical flux functions we use the CIR numerical flux

$$\mathcal{F}(u^-, u^+) = \frac{1}{2}(f(u^-) + f(u^+)) - \frac{\alpha}{2}(u^+ - u^-), \quad \alpha = \left| \frac{\partial f}{\partial u} \left(\frac{u^- + u^+}{2} \right) \right|.$$

331 The integral of the source term (3.4) can be explicitly discretized using a second
 332 order quadrature rule, for example the midpoint rule:

$$333 \quad (3.5) \quad \int_{I_i} h(u) ds \approx |I_i| h(\bar{u}_i).$$

335 Finally, the diffusion terms in (3.3) can be approximated as

$$336 \quad g(u_s(s_{i+1/2})) - g(u_s(s_{i-1/2})) \approx g\left(\frac{\bar{u}_{i+1} - \bar{u}_i}{|I_i|}\right) - g\left(\frac{\bar{u}_i - \bar{u}_{i-1}}{|I_i|}\right).$$

337

338 **3.2. Time discretization. IMEX Runge-Kutta.** After performing the spa-
 339 tial semi-discretization of equation (3.1) we obtain a stiff ODE system of the form

340 (3.6)
$$\frac{\partial U}{\partial t} + F(U) = S(U),$$

341 where $U = (\bar{u}_i(t))$ and $F, S : \mathbb{R}^N \rightarrow \mathbb{R}^N$, being F the non-stiff term and S the stiff one.
 342 An IMEX scheme consists of applying an implicit discretization to the stiff term and
 343 an explicit one to the non stiff term. In this way, both can be solved simultaneously
 344 with high order accuracy using the same *time step* of the convective part, which is in
 345 general much larger than the time step of the diffusive part.

346 When IMEX is applied to system (3.6) it takes the form

347 (3.7)
$$U^{(k)} = U^n - \Delta t \sum_{l=1}^{k-1} \tilde{a}_{kl} F(t_n + \tilde{c}_l \Delta t, U^{(l)}) + \Delta t \sum_{l=1}^{\rho} a_{kl} S(t_n + c_l \Delta t, U^{(l)}),$$

348 (3.8)
$$U^{n+1} = U^n - \Delta t \sum_{k=1}^{\rho} \tilde{\omega}_k F(t_n + \tilde{c}_k \Delta t, U^{(k)}) + \Delta t \sum_{k=1}^{\rho} \omega_k S(t_n + c_k \Delta t, U^{(k)}),$$

 349

350 where $U^n = (\bar{u}_i^n)$, $U^{n+1} = (\bar{u}_i^{n+1})$ are the vector of the unknowns cell averages at
 351 times t^n and t^{n+1} , thus $U^{(k)}$ and $U^{(l)}$ are the vector of unknowns at the stages k, l of
 352 the IMEX method. The matrices $\tilde{A} = (\tilde{a}_{kl})$, with $\tilde{a}_{kl} = 0$ for $l \geq k$, and $A = (a_{kl})$ are
 353 square matrices of order ρ , such that the ensuing scheme is implicit in S and explicit
 354 in F . Solving efficiently at each time step the system of equations corresponding to
 355 the implicit part is extremely important. Therefore, one usually considers $a_{kl} = 0$,
 356 for $l > k$, the so-called diagonally implicit Runge-Kutta (DIRK) schemes .

357 IMEX Runge-Kutta schemes can be represented by a double tableau in the usual
 358 Butcher notation,

359
$$\begin{array}{c|c} \tilde{c} & \tilde{A} \\ \hline & \tilde{\omega} \end{array}, \quad \begin{array}{c|c} c & A \\ \hline & \omega \end{array},$$

360 where $\tilde{w} = (\tilde{w}_1, \dots, \tilde{w}_\rho)$ and $w = (w_1, \dots, w_\rho)$. Besides, the coefficient vectors $\tilde{c} =$
 361 $(\tilde{c}_1, \dots, \tilde{c}_\rho)^T$ and $c = (c_1, \dots, c_\rho)^T$ are only used for the treatment of non autonomous
 362 systems, and have to satisfy the relations

363 (3.9)
$$\tilde{c}_k = \sum_{l=1}^{k-1} \tilde{a}_{kl}, \quad c_k = \sum_{l=1}^k a_{kl}.$$

364 In this work we will consider the second order IMEX-SSP2(2,2,2) L-stable scheme
 365 (see [21])

366
$$\begin{array}{c|cc} 0 & 0 & 0 \\ 1 & 1 & 0 \\ \hline & 1/2 & 1/2 \end{array} \quad \begin{array}{c|cc} \gamma & \gamma & 0 \\ 1-\gamma & 1-2\gamma & \gamma \\ \hline & 1/2 & 1/2 \end{array} \quad \gamma = 1 - \frac{1}{\sqrt{2}}.$$

367 An explicit time integrator needs extremely small time steps due to the following
 368 stability conditions

369 (3.10) $\eta \frac{\Delta t}{(\Delta s)^2} \leq \frac{1}{2},$ (3.11) $\alpha \frac{\Delta t}{\Delta s} \leq 1,$

370 where $\eta = \left| \frac{\partial g}{\partial u_s} \right|$, $\alpha = \left| \frac{\partial f}{\partial u} \right|$, for all cells I_i and for all boundary points $s_{i\pm 1/2}$.
 371 However, IMEX only needs to satisfy the advection stability condition (3.11).

372 **4. Numerical experiments.** In this section the accuracy and convergence of
 373 the proposed numerical scheme is assessed. The developed numerical method is ap-
 374 plied to the discretization and solution of the one and two dimensional financial PDEs
 375 discussed in Section 2. More precisely, experiments under the Black-Scholes model
 376 for vanilla, butterfly and barrier options are presented in Section 4.1. Besides, the
 377 numerical results are compared with the analytical solutions presented in Section 2.
 378 Later, in Section 4.2 two dimensional problems in space are solved. Indeed, Asian
 379 options are priced.

380 At each one of the following subsections, we start by writing the involved PDE in
 381 conservative form. Then, graphs containing numerical results, such as option prices,
 382 Greeks (Delta and Gamma) and numerical errors are presented. Moreover, tables for
 383 the L_1 errors and the L_1 orders of convergence are shown. Additionally, a comparison
 384 of the time step sizes supplied by the stability conditions of the explicit and IMEX
 385 Runge-Kutta methods is presented. For all the tests in this paper a CFL of 0.5 is
 386 considered in the stability conditions.

4.1. Options under the Black-Scholes model. First of all, the Black-Scholes
 PDE (2.3) is written in the conservative form (3.1), where the conservative functions
 are given by:

$$f(u) = (\sigma^2 - r + q)su, \quad g(u_s) = \frac{1}{2}\sigma^2 s^2 \frac{\partial u}{\partial s}, \quad h(u) = (\sigma^2 - 2r + q)u.$$

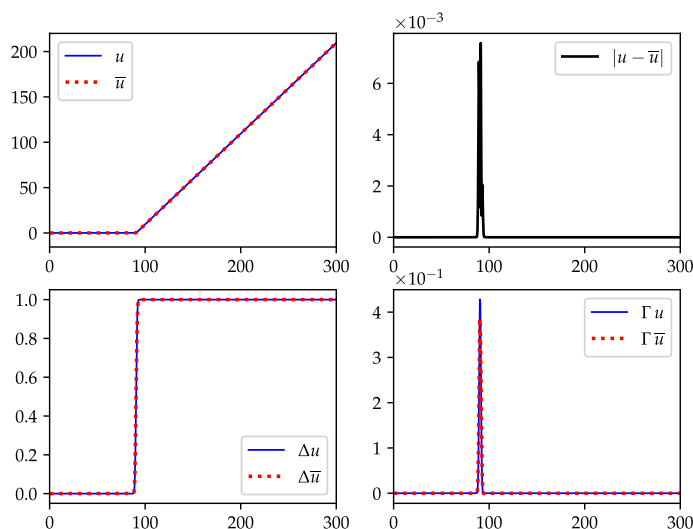
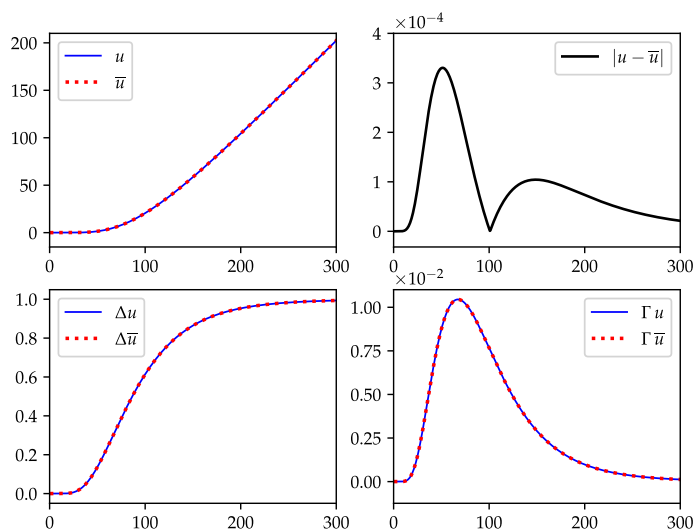
387 Hereafter, vanilla, butterfly and barrier European call options are priced under
 388 this model.

389 **4.1.1. European call options.** In this section, three tests are considered, whose
 390 market data are collected in Table 1. Test 2 is a diffusion-dominated example, while
 391 Test 3 is convection-dominated. Test 1 represents a balanced configuration. Although
 392 the setup of Test 3 is financially unrealistic, because of the high value of r , it is use-
 393 ful as a stress-test of the numerical scheme. In these three experiments the spatial
 394 domain is set to $[0, \bar{s} = 400]$.

	σ	r	q	T	K
Test 1	0.01	0.10	0	1	100
Test 2	0.5	0.02			
Test 3	0.02	0.5			

Table 1: Market data for European call options under the Black-Scholes model.

395 In Figures 1, 2 and 3, numerical (\bar{u}) and exact (u) option prices are plotted at
 396 $t = T$ for Tests 1, 2 and 3, respectively. A mesh with 800 discretization points in space
 397 was considered. Numerical prices were computed with the IMEX Runge-Kutta time
 398 integrator. Besides, numerical errors ($|u - \bar{u}|$) are displayed in that figures. In addition,
 399 exact and numerical Delta and Gamma Greeks at the final time T are presented.
 400 The numerical Greeks ($\Delta\bar{u}$, $\Gamma\bar{u}$) are computed with second order finite differences
 401 approximations, even at the boundaries of the spatial domain, see [11] for details.
 402 The numerical results are plotted in red squares, while the analytical solutions are
 403 represented in continuous blue line. The reader can observe that the proposed finite
 404 volume numerical scheme offers high-resolution approximations, without oscillations,
 405 for the option prices and the Greeks, even at regions of discontinuities and non-
 406 smoothness in the initial condition.

Fig. 1: Call option prices, numerical errors and Greeks (Δ , Γ) for Test 1 at $t = T$.Fig. 2: Call option prices, numerical errors and Greeks (Δ , Γ) for Test 2 at $t = T$.

407 Tables 2, 3 and 4 record L_1 errors and L_1 orders of convergence at $t = T$ for both
 408 explicit and IMEX finite volume numerical methods for Tests 1, 2 and 3, respectively.
 409 L_1 error is given by $L_1 = \Delta s \sum_{i=1}^N |\bar{u}(s_i, T) - u(s_i, T)|$, where N denotes the number
 410 of discretization points in space. Besides, the time steps and execution times are
 411 shown for each spatial discretization. The time steps for IMEX and the explicit
 412 method were obtained from the stability conditions (3.10) and (3.11). Codes were
 413 implemented using C++ programming language, compiled with GNU C++ compiler
 414 9.3.0 and run in a machine with one AMD Ryzen 9 5950X processor. On the one
 415 hand, these tables show that both IMEX and explicit numerical schemes are able to

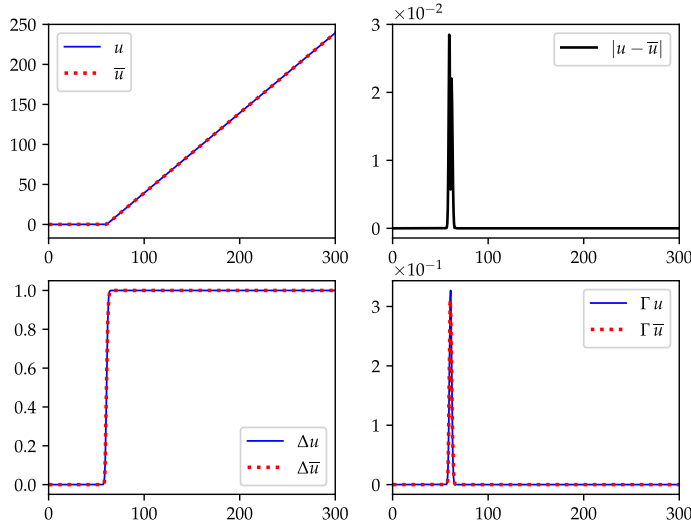


Fig. 3: Call option prices, numerical errors and Greeks (Δ , Γ) for Test 3 at $t = T$.

416 approximate the solution with order two. Second order is achieved even in the presence
 417 of non-smoothness in the initial condition, thus avoiding the necessity of regularization
 418 techniques for the initial condition, like the Rannacher time-stepping. On the other
 419 hand, numerical results show, as expected, that the IMEX time integrator outperforms
 420 the explicit method. In fact, in the diffusion dominated scenario of Test 2, IMEX time
 421 steps are between 54 and 6967 times larger than corresponding explicit time steps.
 422 As a result, IMEX is between 17 and 1791 times faster than the explicit method.
 423 In Figure 4 the natural logarithms of L_1 errors and execution times of Table 3 are
 424 plotted for both the IMEX and explicit numerical schemes; IMEX superiority in this
 425 figure is overwhelming. As expected, when N increases the distance between both
 426 schemes is larger and larger. In advection dominated scenarios, like the one in Test
 427 3, both IMEX and the explicit methods perform similarly in the coarser meshes in
 428 space. Nevertheless, IMEX performs again better when dealing with finer grids in
 429 space. For example, in the mesh with 6400 finite volumes, IMEX time step is 5 times
 430 larger than the corresponding explicit time step, thus executing 1.64 times faster. In
 431 more balanced scenarios, like the one in Test 1, IMEX keeps performing better and
 432 better as long as the space grid is refined in space. In fact, in the grid with $N = 6400$,
 433 IMEX time step is 6.4 times larger than the explicit time step. As a result, IMEX
 434 is able to compute the solution 1.74 times faster. Having in mind that the common
 435 situation in finance is the diffusion dominated scenario, the IMEX time integrator
 436 represents the right choice. As a summary, although both time marching methods
 437 achieve similar results in terms of accuracy and convergence order, IMEX is able to
 438 converge using much larger times steps, thus it consumes much less computing time.

439 **4.1.2. Butterfly Spread.** In this section a butterfly spread option is priced
 440 considering the market data $\sigma = 0.2$, $r = 0.1$, $q = 0$, $T = 0.5$, $K_1 = 45$ and $K_3 = 80$.
 441 The computational domain is set as $[0, \bar{s} = 200]$.

442 In Figure 5, prices, numerical errors and Greeks are shown at $t = T$ with $N =$
 443 800. These plots show that the here proposed numerical methods achieve very good

IMEX				
N	L_1 error	Order	Δt	Time (s)
50	1.6145×10^1	--	1.01×10^{-1}	2.8×10^{-4}
100	7.1629×10^0	1.17	5.03×10^{-2}	4.7×10^{-4}
200	2.6877×10^0	1.41	2.50×10^{-2}	1.18×10^{-3}
400	9.1734×10^{-1}	1.55	1.25×10^{-2}	3.6×10^{-3}
800	2.8046×10^{-1}	1.70	6.26×10^{-3}	1.1×10^{-2}
1600	7.2788×10^{-2}	1.95	3.13×10^{-3}	2.6×10^{-2}
3200	1.7410×10^{-2}	2.06	1.56×10^{-3}	9.5×10^{-2}
6400	3.4791×10^{-3}	2.32	7.82×10^{-4}	3.5×10^{-1}
Explicit				
N	L_1 error	Order	Δt	Time (s)
50	1.6146×10^1	--	1.01×10^{-1}	1.1×10^{-4}
100	7.1626×10^0	1.17	5.03×10^{-2}	1.9×10^{-4}
200	2.6875×10^0	1.41	2.50×10^{-2}	4.4×10^{-4}
400	9.1713×10^{-1}	1.55	1.25×10^{-2}	1.5×10^{-3}
800	2.8039×10^{-1}	1.71	6.26×10^{-3}	4.3×10^{-3}
1600	7.3346×10^{-2}	1.93	1.95×10^{-3}	2.2×10^{-2}
3200	1.7622×10^{-2}	2.06	4.88×10^{-4}	9.6×10^{-2}
6400	3.5252×10^{-3}	2.32	1.22×10^{-4}	6.1×10^{-1}

Table 2: L_1 errors and L_1 orders of convergence of the IMEX and explicit finite volume methods for the call option of Test 1.

IMEX				
N	L_1 error	Order	Δt	Time (s)
50	7.8413×10^0	--	4.34×10^{-2}	3.8×10^{-4}
100	1.9886×10^0	1.98	2.17×10^{-2}	7.8×10^{-4}
200	5.0056×10^{-1}	1.99	1.09×10^{-2}	2.2×10^{-3}
400	1.2554×10^{-1}	1.99	5.43×10^{-3}	6.9×10^{-3}
800	3.1367×10^{-2}	2.00	2.72×10^{-3}	1.5×10^{-2}
1600	7.7625×10^{-3}	2.02	1.36×10^{-3}	5.0×10^{-2}
3200	1.8499×10^{-3}	2.07	6.80×10^{-4}	1.8×10^{-1}
6400	3.7004×10^{-4}	2.32	3.40×10^{-4}	6.7×10^{-1}
Explicit				
N	L_1 error	Order	Δt	Time (s)
50	7.4158×10^0	--	8.00×10^{-4}	6.7×10^{-3}
100	1.8518×10^0	2.00	2.00×10^{-4}	1.8×10^{-2}
200	4.6253×10^{-1}	2.00	5.00×10^{-5}	8.7×10^{-2}
400	1.1551×10^{-1}	2.00	1.25×10^{-5}	4.8×10^{-1}
800	2.8793×10^{-2}	2.00	3.13×10^{-6}	2.9×10^0
1600	7.1211×10^{-3}	2.02	7.81×10^{-7}	2.0×10^1
3200	1.6999×10^{-3}	2.07	1.95×10^{-7}	1.5×10^2
6400	3.4735×10^{-4}	2.29	4.88×10^{-8}	1.2×10^3

Table 3: L_1 errors and L_1 orders of convergence of the IMEX and explicit finite volume methods for the call option of Test 2.

444 approximations of prices and Greeks, even for this butterfly derivative, with sharp
445 corners at strike prices in the initial condition and several jumps in derivatives. In
446 Table 5, L_1 errors and L_1 orders of convergence are shown for this derivative. Second
447 order of convergence is again achieved. IMEX time step is between 33 and 4262 times
448 larger than the explicit time step. As a consequence, IMEX is between 7 and 959
449 times faster.

450 **4.1.3. Barrier Option.** In this section a down-and-out call option with the
451 market data $\sigma = 0.2$, $r = 0.05$, $q = 0$, $T = 1$, $K = 70$ and the barrier at $B = 200$ is
452 priced. The computational domain is thus set to $[B, 5B]$.

453 In Figure 6 option prices, numerical errors, Deltas and Gammas are shown at

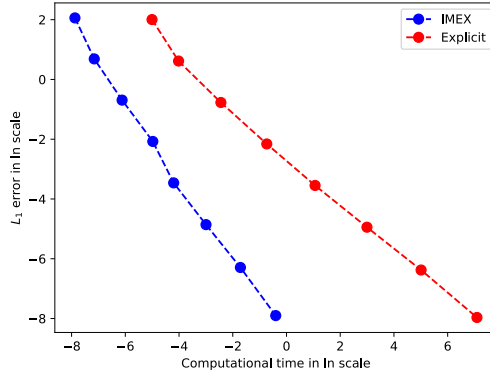


Fig. 4: Efficiency curve of IMEX and explicit time marching schemes for Test 2.

IMEX				
N	L_1 error	Order	Δt	Time (s)
50	3.4261×10^1	—	2.00×10^{-2}	5.8×10^{-4}
100	1.3092×10^1	1.39	1.00×10^{-2}	1.4×10^{-3}
200	4.8437×10^0	1.44	5.00×10^{-3}	4.4×10^{-3}
400	1.6448×10^0	1.56	2.50×10^{-3}	1.2×10^{-2}
800	4.8968×10^{-1}	1.75	1.25×10^{-3}	3.3×10^{-2}
1600	1.2745×10^{-1}	1.94	6.25×10^{-4}	1.1×10^{-1}
3200	3.0473×10^{-2}	2.06	3.13×10^{-4}	4.3×10^{-1}
6400	6.1026×10^{-3}	2.32	1.56×10^{-4}	1.7×10^0
Explicit				
N	L_1 error	Order	Δt	Time (s)
50	3.4278×10^1	—	2.00×10^{-2}	3.5×10^{-4}
100	1.3124×10^1	1.39	1.00×10^{-2}	7.4×10^{-4}
200	4.8616×10^0	1.43	5.00×10^{-3}	1.9×10^{-3}
400	1.6535×10^0	1.56	2.50×10^{-3}	6.3×10^{-3}
800	4.9281×10^{-1}	1.75	1.25×10^{-3}	1.4×10^{-2}
1600	1.2841×10^{-1}	1.94	4.88×10^{-4}	5.3×10^{-2}
3200	3.0728×10^{-2}	2.06	1.22×10^{-4}	3.7×10^{-1}
6400	6.1716×10^{-3}	2.32	3.05×10^{-5}	2.8×10^0

Table 4: L_1 errors and L_1 orders of convergence of the IMEX and explicit finite volume methods for the call option of Test 3.

454 $t = T$ considering a mesh with $N = 800$. These plots show that the here proposed
 455 numerical methods are able to obtain good approximations without oscillations, even
 456 at difficult zones like close to the barrier. Table 6 shows L_1 errors and L_1 order
 457 of convergence at $t = T$. Second order accuracy is achieved again. In this case,
 458 IMEX time step is between 200 and 25606 times larger than the explicit time step.
 459 Consequently, IMEX executes between 10 and 12222 times faster.

460 **4.2. Asian option.** Using the method of lines, the previous one dimensional nu-
 461 merical methods can be easily extended to the two dimensional case. Generally speak-
 462 ing, we are interested in solving the following two dimensional advection-diffusion-
 463 reaction PDE without crossed derivatives:

464 (4.1)
$$\frac{\partial u}{\partial t} + a \frac{\partial u}{\partial x} + b \frac{\partial u}{\partial y} + c \frac{\partial^2 u}{\partial x^2} + d \frac{\partial^2 u}{\partial y^2} + e = 0,$$

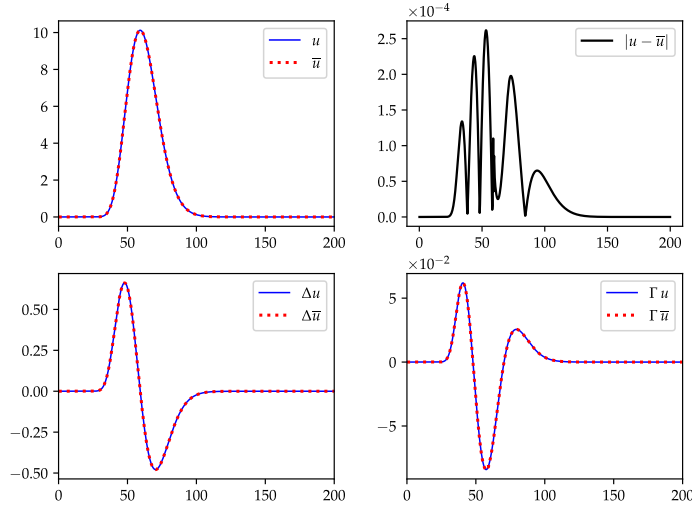


Fig. 5: Butterfly spread option prices, numerical errors and Greeks (Δ, Γ).

IMEX				
N	L_1 error	Order	Δt	Time (s)
50	2.8534×10^0	--	1.66×10^{-1}	9.0×10^{-5}
100	8.6913×10^{-1}	1.72	8.33×10^{-2}	3.1×10^{-4}
200	2.4055×10^{-1}	1.85	4.17×10^{-2}	5.5×10^{-4}
400	6.2948×10^{-2}	1.93	2.08×10^{-2}	1.3×10^{-3}
800	1.6034×10^{-2}	1.97	1.04×10^{-2}	4.1×10^{-3}
1600	4.0019×10^{-3}	2.00	5.21×10^{-3}	1.4×10^{-2}
3200	9.5613×10^{-4}	2.07	2.60×10^{-3}	2.9×10^{-2}
6400	1.9134×10^{-4}	2.32	1.30×10^{-3}	9.9×10^{-2}
Explicit				
N	L_1 error	Order	Δt	Time (s)
50	3.6096×10^0	--	5.00×10^{-3}	6.5×10^{-4}
100	1.0029×10^0	1.85	1.25×10^{-3}	2.7×10^{-3}
200	2.7238×10^{-1}	1.88	3.15×10^{-4}	1.1×10^{-2}
400	7.0883×10^{-2}	1.94	7.81×10^{-5}	4.7×10^{-2}
800	1.7997×10^{-2}	1.98	1.95×10^{-5}	2.5×10^{-1}
1600	4.4939×10^{-3}	2.00	4.88×10^{-6}	1.7×10^0
3200	1.0839×10^{-3}	2.05	1.23×10^{-6}	1.2×10^1
6400	2.2739×10^{-4}	2.25	3.05×10^{-7}	9.5×10^1

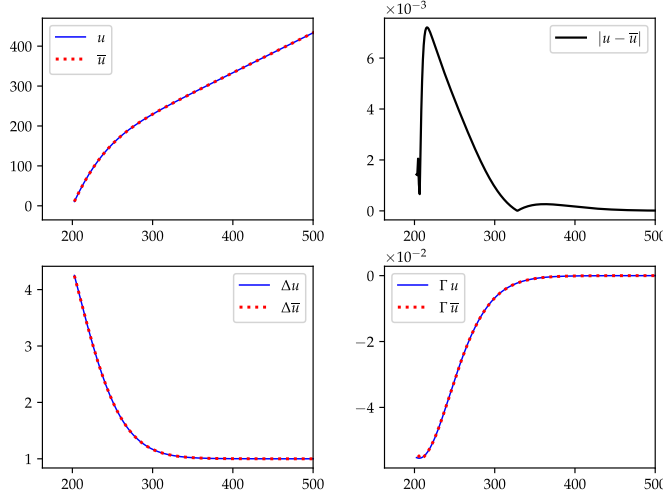
Table 5: L_1 errors and L_1 orders of convergence of the IMEX and explicit finite volume methods for the butterfly spread option.

465 where a, b, c, d, e are functions of t, x, y and u . This equation (4.1) can be written in
 466 conservative form as

467 (4.2)
$$\frac{\partial u}{\partial t} + \frac{\partial f_1}{\partial x}(u) + \frac{\partial f_2}{\partial y}(u) = \frac{\partial g_1}{\partial x}(u_x) + \frac{\partial g_2}{\partial y}(u_y) + h(u).$$

468 The stability conditions are

469 (4.3)
$$2\eta_1 \frac{\Delta t}{(\Delta x)^2} + 2\eta_2 \frac{\Delta t}{(\Delta y)^2} \leq \frac{1}{2}, \quad \alpha_1 \frac{\Delta t}{\Delta x} + \alpha_2 \frac{\Delta t}{\Delta y} \leq 1,$$

Fig. 6: Down-and-out call option prices, numerical errors and Greeks (Δ , Γ) at $t = T$.

IMEX				
N	L_1 error	Order	Δt	Time (s)
50	1.3889×10^2	--	1.00×10^0	1.8×10^{-4}
100	3.4052×10^1	2.03	5.00×10^{-1}	2.6×10^{-4}
200	8.5310×10^0	2.03	2.50×10^{-1}	4.6×10^{-4}
400	2.1249×10^0	2.02	1.25×10^{-1}	9.4×10^{-4}
800	5.2912×10^{-1}	2.01	6.25×10^{-2}	2.4×10^{-3}
1600	1.3097×10^{-1}	1.98	3.13×10^{-2}	7.3×10^{-3}
3200	3.1547×10^{-2}	2.00	1.56×10^{-2}	1.6×10^{-2}
6400	6.7624×10^{-3}	2.26	7.81×10^{-3}	4.5×10^{-2}
Explicit				
N	L_1 error	Order	Δt	Time (s)
50	1.3979×10^2	--	5.00×10^{-3}	1.8×10^{-3}
100	3.4401×10^1	2.02	1.25×10^{-3}	7.7×10^{-3}
200	8.5373×10^0	2.01	3.12×10^{-4}	3.0×10^{-2}
400	2.1271×10^0	2.01	7.81×10^{-5}	1.3×10^{-1}
800	5.3130×10^{-1}	2.01	1.95×10^{-5}	9.5×10^{-1}
1600	1.3316×10^{-1}	2.01	4.88×10^{-6}	6.4×10^0
3200	3.3721×10^{-2}	2.05	1.22×10^{-6}	6.4×10^1
6400	8.8809×10^{-3}	2.22	3.05×10^{-7}	5.5×10^2

Table 6: L_1 errors and L_1 orders of convergence of the IMEX and explicit finite volume methods for the down-and-out call option.

470 where $\eta_1 = \left| \frac{\partial g_1}{\partial u_x} \right|$, $\eta_2 = \left| \frac{\partial g_2}{\partial u_y} \right|$, $\alpha_1 = \left| \frac{\partial f_1}{\partial u} \right|$ and $\alpha_2 = \left| \frac{\partial f_2}{\partial u} \right|$ for all boundaries of all
471 volumes.

472 Therefore, the Asian PDE (2.13) is then written in the conservative form of PDE
473 (4.2) using

$$474 \quad f_1(u) = (\sigma^2 - r)su, \quad f_2(u) = -\frac{1}{T-t}(s-a)u,$$

$$475 \quad g_1(u_s) = \frac{1}{2}\sigma^2 s^2 u_s, \quad g_2(u_a) = 0, \quad h(u) = \left(\sigma^2 - 2r + \frac{1}{T-t} \right) u.$$

476 At this point, a fixed strike Asian call option is valued with the market data $\sigma = 0.2$,
 477 $r = 0.1$, $T = 1$, $K = 100$ on the spatial domain $(s, a) \in [0, 300] \times [0, 300]$. Numerical
 478 option prices and Greeks at $t = T$ using a mesh of size $N_1 \times N_2 = 800 \times 800$ are shown
 479 in Figure 7.

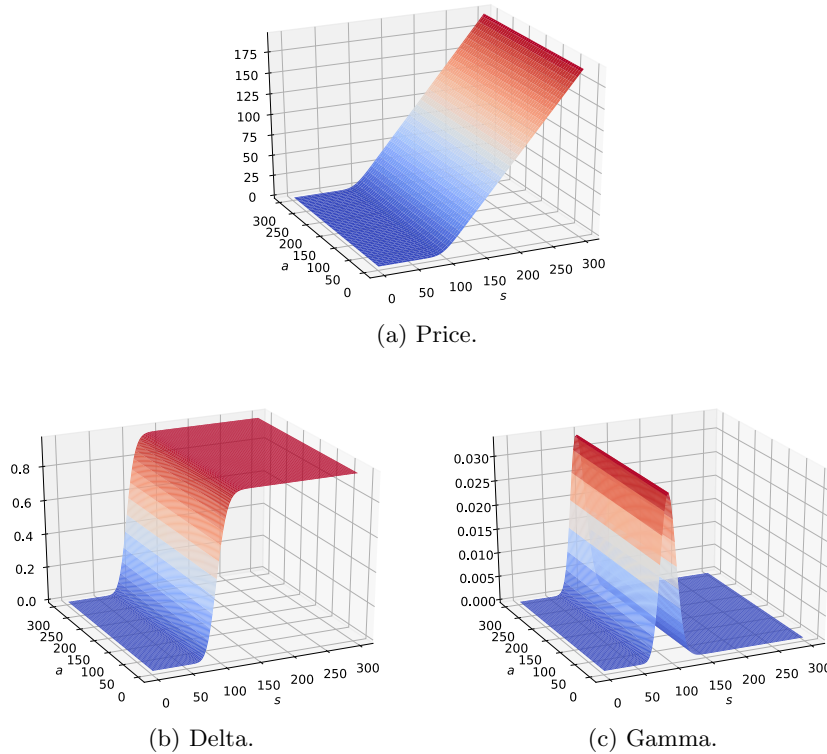


Fig. 7: Prices, Deltas and Gammas of the Asian option at $t = T$.

480 Table 7 records L_1 errors and L_1 orders of convergence at $t = \frac{T}{2}$. Both IMEX and
 481 explicit numerical schemes achieve second-order accuracy in the L_1 norm. In this case
 482 f_2 depends on time t . Therefore, the time step inferred by the convective stability
 483 condition in (4.3) depends on the actual time step. For each row of the table, only
 484 the smallest time step is shown, i.e the one computed at the final time step. In the
 485 case of this financial derivative, IMEX time marching is up to 40 times faster than
 486 the explicit scheme.

487 **5. Conclusions.** In this article we have shown that finite volume IMEX Runge-
 488 Kutta numerical schemes are remarkably suitable for solving PDE option pricing
 489 problems. On the one hand, the IMEX time discretization is outstandingly efficient.
 490 Indeed, large time steps can be used, avoiding the need to use the smaller, and possibly
 491 extremely small, time steps enforced by the diffusion stability condition, which has to
 492 be satisfied in explicit schemes. Numerical results show that IMEX outperforms the
 493 explicit method. In fact, IMEX is the only way to solve problems in highly refined
 494 meshes is space. Besides, even in its worst scenarios, IMEX performs at least as well as

IMEX				
$N_1 \times N_2$	L_1 error	Order	Δt	Time (s)
25×25	2.6092×10^4	--	1.00×10^{-2}	1.7×10^{-2}
50×50	8.5678×10^3	1.61	5.00×10^{-3}	8.0×10^{-2}
100×100	8.5678×10^3	1.42	2.50×10^{-3}	5.9×10^{-1}
200×200	1.2092×10^3	1.40	1.25×10^{-3}	5.7×10^0
400×400	3.2323×10^2	1.90	6.25×10^{-4}	5.3×10^1
800×800	9.7991×10^1	1.72	3.13×10^{-4}	5.1×10^2
1600×1600	2.3879×10^1	2.04	1.57×10^{-4}	5.0×10^3
Explicit				
$N_1 \times N_2$	L_1 error	Order	Δt	Time (s)
25×25	2.6273×10^4	--	1.00×10^{-2}	8.1×10^{-3}
50×50	8.5704×10^3	1.62	5.00×10^{-3}	3.5×10^{-2}
100×100	2.9837×10^3	1.52	1.25×10^{-3}	2.3×10^{-1}
200×200	9.8509×10^2	1.59	3.12×10^{-4}	4.1×10^0
400×400	3.2357×10^2	1.61	7.81×10^{-5}	6.6×10^1
800×800	9.8241×10^1	1.72	1.95×10^{-5}	1.2×10^3
1600×1600	2.4234×10^1	2.02	4.88×10^{-6}	2.0×10^5

Table 7: L_1 errors and L_1 orders of convergence of the IMEX and explicit finite volume methods for the Asian option.

495 the explicit method. On the other hand, finite volume space discretization contributes
 496 substantially to the achievement of second order convergence. Its consideration is
 497 crucial to handle appropriately convection dominated problems and/or problems with
 498 non smooth initial and/or boundary conditions, which is the usual situation in finance.
 499 Thus, no special regularization techniques of the non smooth data need to be taken
 500 into account. The accuracy of the numerical scheme turns to be of key importance
 501 for the accurate and non oscillatory computation of the Greeks. Finally, in this paper
 502 we provide a set of benchmark problems, together with their analytical solutions.
 503 These benchmarks can also be valuable for mathematical researchers working in the
 504 development of high order numerical schemes for advection-diffusion problems.

505

REFERENCES

- 506 [1] Y. ACHDOU AND O. PIRONNEAU, *Frontiers in Applied Mathematics. Computational Methods*
 507 *for Option Pricing*, SIAM, 2005.
- 508 [2] ALFREDO BERMÚDEZ AND MARÍA R. NOGUEIRAS AND CARLOS VÁZQUEZ, *Numerical analysis*
 509 *of convection-diffusion-reaction problems with higher order characteristics finite elements.*
 510 *Part I: Time discretization*, SIAM Journal on Numerical Analysis, 44 (2006), pp. 1829–
 511 1853.
- 512 [3] O. BHATOO, A. A. I. PEER, E. TADMOR, D. Y. TANGMAN, AND A. A. E. F. SAIB, *Conservative*
 513 *third-order central-upwind schemes for option pricing problems*, Vietnam Journal of
 514 Mathematics, 47 (2019), pp. 813–8332.
- 515 [4] O. BHATOO, A. A. I. PEER, E. TADMOR, D. Y. TANGMAN, AND A. A. E. F. SAIB, *Efficient*
 516 *conservative second-order central-upwind schemes for option-pricing problems*, Journal of
 517 Computational Finance, 22 (2019), pp. 39–78.
- 518 [5] F. BLACK AND M. SCHOLES, *The Pricing of Options and Corporate Liabilities*, The Journal of
 519 Political Economy, 81 (1973), pp. 637–654.
- 520 [6] S. BOSCARINO AND G. RUSSO, *On a Class of Uniformly Accurate IMEX RungeKutta Schemes*
 521 *and Applications to Hyperbolic Systems with Relaxation*, SIAM Journal on Scientific Com-
 522 puting, 31 (2009), pp. 1926–1945.
- 523 [7] D. CASTILLO, A. FERREIRO, J. GARCA-RODRIGUEZ, AND C. VZQUEZ, *Numerical methods to*
 524 *solve PDE models for pricing business companies in different regimes and implementation*
 525 *in GPUs*, Applied Mathematics and Computation, 219 (2013), pp. 11233 – 11257.
- 526 [8] Y. D'HALLUIN, P. A. FORSYTH, AND G. LABAHN, *A Semi-Lagrangian Approach for American*
 527 *Asian Options under Jump Diffusion*, SIAM Journal on Scientific Computing, 27 (2006),

- 528 pp. 315–345.
- 529 [9] D. DUFFY, *Finite Difference Methods in Financial Engineering: A Partial Differential Equa-*
530 *tion Approach*, Wiley, 2006.
- 531 [10] D. J. DUFFY, *Exponentially fitted difference schemes for barrier options*, in *Finite Difference*
532 *Methods in Financial Engineering: A Partial Differential Equation Approach*, John Wiley
533 & Sons, Ltd, 2013, ch. 14, pp. 153–163.
- 534 [11] B. FORNBERG, *Generation of Finite Difference Formulas on Arbitrarily Spaced Grids*, *Mathe-*
535 *matics of Computation*, 51(184) (1988), pp. 699–706.
- 536 [12] K. J. I. T. HOUT AND S. FOULON, *ADI finite difference schemes for option pricing in the*
537 *Heston model with correlation*, *International Journal of Numerical Analysis and Modeling*,
538 7 (2010), pp. 303–320.
- 539 [13] J. E. INGERSOLL, *Theory of Financial Decision Making*, Rowman & Littlefield, 1987.
- 540 [14] A. KURGANOV AND D. LEVY, *A Third-Order Semidiscrete Central Scheme for Conservation*
541 *Laws and Convection-Diffusion Equations*, *SIAM Journal on Scientific Computing*, 22
542 (2000), pp. 1461–1488.
- 543 [15] A. KURGANOV AND E. TADMOR, *New high-resolution central schemes for nonlinear conservation*
544 *laws and convectiondiffusion equations*, *Journal of Computational Physics*, 160 (2000),
545 pp. 241 – 282.
- 546 [16] L.C.G. ROGERS AND Z. SHI, *The Value of an Asian option*, *Journal of Applied Probability*, 32
547 (1995), pp. 1077–1088.
- 548 [17] D. LEVY, G. PUPPO, AND G. RUSSO, *Compact central WENO schemes for multidimensional*
549 *conservation laws*, *SIAM Journal on Scientific Computing*, 22 (2000), pp. 656–672.
- 550 [18] M. LUSKIN, R. RANNACHER, AND W. WENDLAND, *On the Smoothing Property of the Crank-*
551 *Nicolson scheme*, *Applicable Analysis*, 14 (1982), pp. 117–135.
- 552 [19] R. C. MERTON, *Theory of Rational Option Pricing*, *The Bell Journal of Economics and Man-*
553 *agement Science*, 4 (1973), pp. 141–183.
- 554 [20] H. NESSYAHU AND E. TADMOR, *Non-oscillatory central differencing for hyperbolic conservation*
555 *laws*, *Journal of Computational Physics*, 87 (1990), pp. 408–463.
- 556 [21] L. PARESCHI AND G. RUSSO, *ImplicitExplicit RungeKutta Schemes and Applications to Hyper-*
557 *bolic Systems with Relaxation*, *Journal of Scientific Computing*, 25 (2005), pp. 129–155.
- 558 [22] A. PASCUCCI, *PDE and Martingale Methods in Option Pricing*, Springer, 2011.
- 559 [23] G. I. RAMÍREZ-ESPINOZA AND M. EHRHARDT, *Conservative and Finite Volume Methods for the*
560 *Convection-Dominated Pricing Problem*, *Advances in Applied Mathematics and Mechan-*
561 *ics*, 5 (2013), p. 759790.
- 562 [24] D. RICH, *The Mathematical Foundations of Barrier Option Pricing Theory*, *Advances in Fu-*
563 *tures and Options Research*, 7 (1994), pp. 267–311.
- 564 [25] M. RUBINSTEIN AND E. REINER, *Breaking down the barriers*, *Risk*, 4 (1991), pp. 28–35.
- 565 [26] J. R. M. RMAN, *Analytical Finance: Volume I and II: The Mathematics of Equity Derivatives,*
566 *Markets, Risk and Valuation*, Palgrave Macmillan, 2017.
- 567 [27] S. E. SHREVE, *Stochastic Calculus for Finance*, Springer, 2004.
- 568 [28] B. WADE, A. KHALIQ, M. YOUSUF, J. VIGO-AGUIAR, AND R. DEININGER, *On smoothing of the*
569 *CrankNicolson scheme and higher order schemes for pricing barrier options*, *Journal of*
570 *Computational and Applied Mathematics*, 204 (2007), pp. 144 – 158.
- 571 [29] P. WILMOTT, *Paul Wilmott on Quantitative Finance*, Wiley, 2006.
- 572 [30] P. ZHANG, *Exotic Options*, World Scientific, 2nd ed., 1998.
- 573 [31] R. ZVAN, P. A. FORSYTH, AND K. R. VETZAL, *Robust numerical methods for PDE models of*
574 *Asian options*, *Journal of Computational Finance*, 1 (1997), pp. 39–78.
- 575 [32] R. ZVAN, P. A. FORSYTH, AND K. R. VETZAL, *A finite volume approach for contingent claims*
576 *valuation*, *IMA Journal of Numerical Analysis*, 21 (2001), pp. 703–731.